Genes & Diseases (2021) 8, 232–240

Available online at www.sciencedirect.com

ScienceDirect

journal homepage: http://ees.elsevier.com/gendis/default.asp

FULL LENGTH ARTICLE

Depletion of *VPS35* attenuates metastasis of hepatocellular carcinoma by restraining the Wnt/PCP signaling pathway

Yi Liu [a,1], Haijun Deng [a,1], Li Liang [a], Guiji Zhang [a], Jie Xia [a], Keyue Ding [b], Ni Tang [a,**], Kai Wang [a,*]

[a] *Key Laboratory of Molecular Biology for Infectious Diseases (Ministry of Education), Institute for Viral Hepatitis, Department of Infectious Diseases, The Second Affiliated Hospital, Chongqing Medical University, Chongqing, 400016, PR China*
[b] *Department of Bioinformatics, School of Basic Medicine, Chongqing Medical University, Chongqing, 400016, PR China*

Received 17 February 2020; received in revised form 10 July 2020; accepted 16 July 2020
Available online 25 July 2020

KEYWORDS
Epithelial–mesenchymal transition;
Hepatocellular carcinoma (HCC);
Metastasis;
Retromer complex;
VPS35;
Wnt/PCP signaling pathway

Abstract Vesicle Protein Sorting 35 (VPS35) is a novel oncogene that promotes tumor growth through the PI3K/AKT signaling in hepatocellular carcinoma (HCC). However, the role of VPS35 in HCC metastasis and the underlying mechanisms remain largely unclear. In this study, we observed that overexpression of VPS35 enhanced hepatoma cell invasion and metastasis by inducing epithelial–mesenchymal transition (EMT)-related gene expression. Conversely, knockout of VPS35 significantly inhibited hepatoma cell migration and invasion. Furthermore, depletion of VPS35 decreased the lung metastasis of HCC in nude mice. By transcriptome analysis, we determined that VPS35 promoted HCC metastasis by activating the Wnt/non-canonical planar cell polarity (PCP) pathway. Mechanistically, VPS35 activated the PCP pathway by regulating membrane sorting and trafficking of Frizzled-2 (FZD2) and ROR1 in hepatoma cells. Collectively, our results indicate that VPS35 promotes HCC metastasis via enhancing the Wnt/PCP signaling, thus providing a potential prognostic marker and therapeutic target for HCC.

* Corresponding author.
** Corresponding author.
E-mail addresses: nitang@cqmu.edu.cn (N. Tang), wangkai@cqmu.edu.cn (K. Wang).
Peer review under responsibility of Chongqing Medical University.
[1] These authors contributed equally to this work.

https://doi.org/10.1016/j.gendis.2020.07.009

Introduction

Hepatocellular carcinoma (HCC) is the most common type of primary malignant liver cancer, and constitutes a serious medical problem worldwide.[1] With 841,000 new cases diagnosed and almost 782,000 deaths caused in 2018, HCC is estimated to be the sixth most frequently diagnosed cancer and is the fourth leading cause of cancer-related death globally.[2] Despite the advances in diagnostic methods and surgical treatment, the overall 5-year survival rate remains poor.[3] Metastasis and recurrence are the major causes of mortality in patients with HCC.[4] Therefore, novel tools and approaches are needed to uncover new molecular mechanisms underlying HCC metastasis, and to identify novel therapeutic and diagnostic strategies to treat and prevent metastases.

The planar cell polarity (PCP) pathway is a non-canonical Wnt signaling pathway triggered by binding of Wnt ligand to its Frizzled (Fzd) receptor.[5] The conserved PCP core components include specific Wnt ligands (usually Wnt5A, 5B, 7, and 11 in mammals), members of the Fzd receptor family, and co-receptors (such as Ror1/2, Ptk7, Ryk, Dachsous, and Fat). Binding of Wnt ligands leads to recruitment of Disheveled to Wnt/PCP Fzd receptors and activation of small GTPases of the Rho family (including Rac1, RhoA, and Cdc42), which are implicated in cytoskeleton remodeling and cell contractility, and the p62/JNK pathway.[6] PCP signaling pathway plays a pivotal role in maintaining polarized epithelial tissue structure and promoting migration, convergence, and extension during development.[7] Although previously overlooked, several studies have recently uncovered important contributions of the PCP pathway to tumor malignancy.[8] Wnt/PCP components are upregulated in melanoma and cancer of the breast, ovary, and pancreas, and their upregulation is associated with poor prognosis.[9,10] A recent study showed that FRIZZLED-7 and other Wnt/PCP components are upregulated in ovarian cancer cells, promoting cell proliferation, cell migration, and stemness in part via RhoA activity.[11]

Vesicle Protein Sorting 35 (VPS35) protein — a core component of the retromer complex — is involved in retrograde transport from the endosome to the plasma membrane or the trans-Golgi network (TGN).[12] The retromer complex is essential for the maintenance of neurons. Impaired retromer function has been implicated in human neurodegenerative diseases, including Parkinson's disease and Alzheimer's disease.[13] A recent study suggested that VPS35 silencing promoted association of N-Ras with cytoplasmic vesicles, attenuated GTP loading of Ras, and inhibited mitogen-activated protein kinase (MAPK) signaling and growth of N-Ras–dependent melanoma cells.[14] Although the role of VPS35 in neurodegenerative diseases has been well documented, much less is known about its role in cancer.

In our previous study, we performed whole-exome and RNA sequencing in a small liver hepatocellular carcinoma (LIHC) cohort and characterized the transcriptional pattern of tumor-mutated alleles. We identified VPS35 as a novel oncogene that promotes tumor growth through the PI3K/AKT signaling.[15] In this study, we further explored the function of VPS35 in the metastasis of HCC and elucidated the underlying mechanisms.

Material and methods

Tumor tissue specimens

A total of 40 HCC tumor samples and paired adjacent noncancerous liver tissues were obtained from curative resections at the Second Affiliated Hospital of Chongqing Medical University (Chongqing, PR China) between 2014 and 2017. The study was approved by the Institutional Review Board of Chongqing Medical University.

Antibodies

Antibodies were used as follows: anti-VPS35 (1:10,000, ab157220, Abcam, USA), anti-E-cadherin (1:10,000, ab40772, Abcam, USA), anti-N-cadherin (1:1000, 13116, Cell Signaling Technology, USA), anti-β-actin (1:2000, TA-09, ZSGB-BIO, China), anti-GAPDH (1:2000, AG019, Beyotime, China), anti-ROCK1 (1:500, WL01761, Wanleibio, China), anti-JNK (1:1000, GTX133806, Gene Tex, USA), anti-p-JNK (1:1000, AJ518, Beyotime, China), anti-Na/K ATPase (1:2000, 619736, ZEN BIO, China), anti-Frizzled 2 (1:1000, 24272-1-AP, Proteintech, USA), anti-ROR1 (1 μg/ml, AF2000, R&D system, USA), anti-MMP9 (1:1000, S1241, Bioworld, USA), p62 (1:1000, 5114, Cell Signaling Technology, USA), anti-Rac (1:500, WL02851, Wanleibio, China), anti-RhoA (1:500, WL02853, Wanleibio, China), anti-Rac (1:1000, ab76535, Abcam, USA), anti-RhoA (1:1000, bs-5330R, Bioss, USA), anti-p-p62 (1:1000, GTX128171, Gene Tex, USA), anti-FZD1 (1:1000, GTX108181, Gene Tex, USA).

Cell lines and culture

Human HCC cell lines MHCC-97H, SK-Hep1, and Huh7 were obtained from the Cell Bank of the Chinese Academy of Sciences (Shanghai, China). VPS35-konckout (KO) SK-Hep1 cells were generated by lentiCRISPR system as described previously.[15] Adenoviral recombinant AdVPS35 was generated using the AdEasy system. Green fluorescent protein-expressing analogous adenovirus (AdGFP) was applied as a control. Cells were maintained in DMEM (Hyclone) supplemented with 10% fetal bovine serum (FBS; Gibco, Rockville, MD, USA), 100 mg/ml of streptomycin, and 100 unit/ml of penicillin in a humidified incubator at 37 °C with 5% CO_2 and 95% air.

Immunofluorescence

E-cadherin, N-cadherin, and ROR1 were detected with the relative rabbit polyclonal antibodies. The specific signals were visualized with Alexa Fluor 488 or 594 secondary antibody (Invitrogen). Nuclei were stained with 1 μg/ml DAPI (10236276001, Roche Diagnostics GmbH, Mannheim, Germany) for 3 min. Stained sections were analyzed by a laser scanning confocal microscope (Leica TCS SP8, Solms, Germany).

Wound scratch assay

Cells were grown in 96-well plates until 90% confluent, then the cell surface was scraped with WoundMaker™ to create wounds. Before incubation in a serum-free medium, cells in suspension and debris were removed. After 18—36 h, cells migrating at the front of the wound were photographed by the IncuCyte ZOOM Live-Cell Imaging system (Essen BioScience, Ann Arbor, MI, USA).

Transwell invasion assay

Cell invasion was evaluated using Cell Culture Insert (Transparent PET Membrane 8 μm pore size, 6.5 mm diameter, FALCON, USA). In brief, cells (6×10^4) were washed with PBS, then resuspended in 200 μl of serum-free medium and added to the upper chamber that was coated with Matrigel (BD Biosciences, San Jose, California, USA). At the same time, medium containing 10% FBS was added to the lower chamber. The chambers were incubated in 5% CO_2 at 37 °C for 24 h, then fixed for 15 min with 4% paraformaldehyde (PFA), stained for 3 min with crystal violet, and quantified (ten random 200× fields per well) under Axio Imager A2 (ZEISS, Germany).

RNA extraction, reverse transcription, and quantitative real time-PCR

Total RNA was extracted from HCC cells using TRIzol reagent (Invitrogen, Rockville, MD, USA) according to the manufacturer's instructions. Purified RNA samples were reverse-transcribed into cDNA using the PrimeScript™ RT Reagent Kit with gDNA Eraser (RR047A, TaKaRa, Tokyo, Japan). Quantitative Real-Time PCR analysis of target genes was performed using the SYBR Green qPCR Master Mix (Bio-Rad, Hercules, CA, USA) with specific primers (Table S1). Each sample was analyzed in triplicate. Relative mRNA levels were calculated using the $2^{-\Delta\Delta Ct}$ method using β-actin as the reference gene for normalization.

Western blotting

Cells or liver samples were lysed in cell lysis buffer (Beyotime Biotechnology, Shanghai, China) supplemented with 1 mM of phenylmethanesulfonyl fluoride (Beyotime). Cell-surface and cytoplasmic proteins were extracted using the Membrane and Cytosol Protein Extraction Kit (Cat# P0033, Beyotime) according to the manufacturer's instructions. Total proteins (30 μg) were separated by 10% SDS/PAGE and transferred to polyvinylidene difluoride membranes (Millipore, Billerica, MA, USA). The immunoblots were probed with the indicated antibodies. Protein bands were visualized with Ultra-sensitive chemiluminescence substrate kits (10300, New Cell &Molecular Biotech Co, Ltd, Su Zhou, China). GAPDH or β-actin were used as internal controls. All experiments were independently repeated three times.

RNA-sequencing (RNA-seq) analysis

Total RNA was extracted from parental or VPS35-KO SK-Hep1 cells using TRIzol reagent (Invitrogen, Rockville, MD, USA) according to the manufacturer's instructions. RNA-seq was performed by the Beijing Genomics Institute (BGI, Shenzhen, China). Briefly, strand-specific RNA-seq libraries were prepared using the NEBNext Ultra RNA Library Prep Kit for Illumina (New England Biolabs, Beverly, MA, USA). Six samples were sequenced on a Hiseq 4000 sequencing platform (Illumina, San Diego, CA, USA). We used the bioinformatics pipeline used in our previous study to analyze differential gene expression between VPS35-KO and parental cells. The RNA-seq data were submitted to the Sequence Read Archive (SRA) (https://www.ncbi.nlm.nih.gov/sra) under the number SUB6834808..

Immunohistochemistry

Liver tissue samples were fixed in fresh 4% PFA and embedded in paraffin according to standard procedures. Sections were incubated with the indicated primary antibodies overnight at 4 °C. Subsequently, the slides were incubated with a secondary anti-rabbit or anti-mouse IgG (ZSGB-BIO, Beijing, China) and visualized using 3,3′-diaminobenzidine (ZSGB-BIO). Stained slides were scanned with the MoticEasyScanner (Motic, Hong Kong, China) and images were acquired using Motic DSAssistant Lite (Motic VM V1 Viewer 2.0).

Mouse studies

All animal experiments were performed using 6-week-old athymic nude mice. MHCC-97H cells were harvested using trypsin, washed twice with PBS, and re-suspended in PBS. The suspended cells (2×10^6/200 μl) were injected into the lateral tail vein of male BALB/c nude mice. After 60 days, mice were sacrificed. Lung tissues were fixed in 4% PFA, embedded in paraffin, sectioned at 5 μm thickness, and then stained with hematoxylin and eosin (H&E). A minimum of 15 sections per mouse was examined under a light microscope. All animal experiments were carried out according to the guidelines of the Institutional Animal Care and Use Committee at Chongqing Medical University (project license number: 2017012). Animal care and use protocols adhered to national regulations for the administration of laboratory animals.

Statistical analysis

All data are presented as mean ± standard deviation (SD). GraphPad Prism 7.0 software (La Jolla, CA, USA) was used to perform all statistical analyses and prepare graphs. For statistical analysis, an unpaired, two-tailed *t*-test was applied, unless indicated differently in figure legends. Statistical significance was determined using one-way ANOVA for multiple comparisons. $P < 0.05$ was considered statistically significant.

Results

VPS35 depletion inhibits HCC cell migration and invasion

Cancer cell migration and invasion are crucial events for liver cancer metastasis. Therefore, we first explored the

role of *VPS35* on HCC cell migration and invasion. Compared with L02 cell line, an increased endogenous expression of VPS35 in the majority of hepatoma cell lines rather than in Huh7 and SNU-449 cell lines (Fig. S1A). Wound scratch assays revealed that loss of *VPS35* inhibited migration of MHCC-97H and SK-Hep1 cells (Fig. 1A). Instead, *VPS35*-overexpressing Huh7 cells showed enhanced wound closure (Fig. 1B). Next, invasive capacities were assessed using a transwell assay. As shown in Fig. 1C and D, respectively, *VPS35* knockout in SK-Hep1 cells inhibited cell migration and invasiveness, while *VPS35* overexpression in Huh7 cells had the opposite effect. To assess the role of VPS35 in the colonization potential of hepatoma cells *in vivo*, we injected VPS35-KO and parental MHCC-97H cells into the tail vein of nude mice and analyzed lung metastases after 8 weeks. Fewer lung metastases were found in VPS35-KO-injected mice than in parental MHCC-97H-injected mice (2/9 vs 5/9, respectively; Fig. 1E). These observations were confirmed by H&E staining of lung tissues (Fig. 1F). Taken together, our results suggest that *VPS35* depletion decreased the migratory and invasive abilities of hepatoma cells *in vivo* and *in vitro*.

VPS35 knockout reduces the expression of EMT-related genes in hepatoma cells

Given that the epithelial—mesenchymal transition (EMT) program is critical for migration and invasiveness of most tumor,[16] we next examined whether *VPS35* regulates EMT-related gene expression in HCC cell lines. Quantitative RT-PCR showed that *VPS35* overexpression upregulated the mesenchymal markers *N-cadherin, Vitronectin, Matrix Metallopeptidase 14 (MMP14), Matrix Metallopeptidase 9 (MMP9)* and *Collagen type I alpha 2 (COL1A2)* at the mRNA level. Conversely, *VPS35*-depleted MHCC-97H cells exhibited increased expression of *E-cadherin*, but decreased expression of *N-cadherin, Fibronectin, MMP14*, and *MMP9* (Fig. 2A). Further, Western blot analysis revealed that VPS35 overexpression upregulated MMP9 and N-cadherin, but downregulated E-cadherin. Conversely, E-cadherin was upregulated, while MMP9 and N-cadherin were downregulated in VPS35-depleted MHCC-97H cells (Fig. 2B). Immunofluorescence analysis showed similar results (Fig. 2C). Consistent with the *in vitro* results, downregulation of E-cadherin and upregulation of N-cadherin and

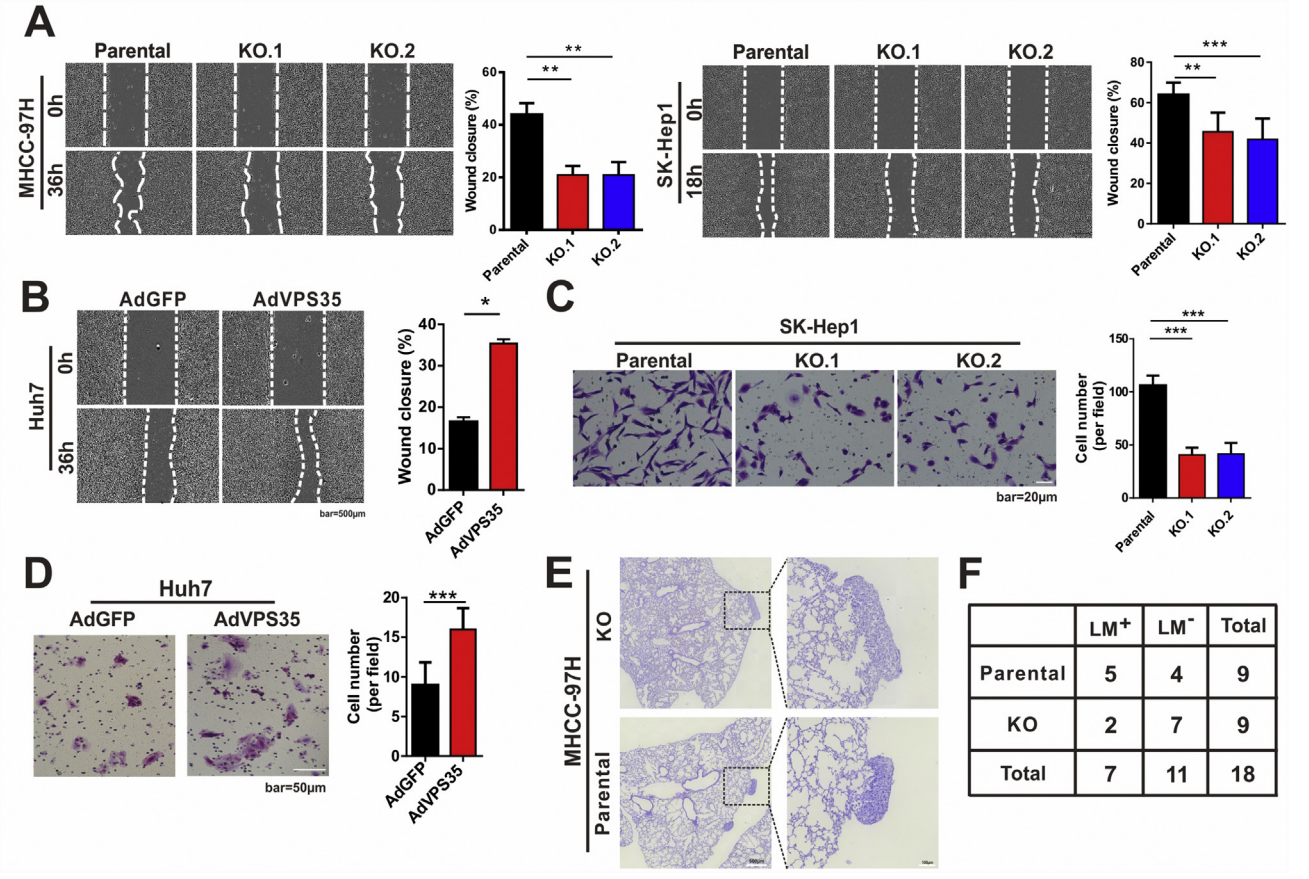

Figure 1 VPS35 depletion inhibits HCC cell migration and invasion. (**A**—**B**) Wound scratch assays performed using the indicated HCC cells (left). Quantification of the wound-scratch assays with the indicated cells (bar graphs; right). Transwell assay with VPS35-KO (Knockout) hepatoma cells (**C**) and VPS35-OE (Overexpressing) Huh7 (**D**). All experiments were performed in triplicate. Data are means ± SD. Statistical significance was determined as $^{*}P < 0.05$, $^{**}P < 0.01$, $^{***}P < 0.001$. (**E**) VPS35-KO and parental MHCC-97H cells (2×10^6/site) were injected into nude mice through the tail vein. Representative staining of lung metastatic tumors ($n = 9$/group) is shown. (**F**) The number of mice with lung metastatic tumors was determined by observation under anatomical microscope, LM, lung metastasis.

MMP9 were also observed in HCC clinical samples (Fig. 2D). These results suggest that *VPS35* silencing inhibited tumor invasion and metastasis by downregulating EMT markers.

Overexpression of *VPS35* activates Wnt/PCP signaling pathway in hepatoma cells

To investigate the molecular mechanism underlying *VPS35*-promoted hepatoma cell invasion and metastasis, we performed RNA-Seq analysis in *VPS35*-KO and parental SK-Hep1 cells. As shown in Fig. 3A and Fig. S1B, the differentially expressed genes (DEGs), which were significantly enriched in the Wnt/PCP signaling (e.g., *Wnt7B*, *AXIN2*, *Rac3*), were notably downregulated in *VPS35*-KO cells. These results were confirmed by qRT-PCR analysis of selected DEGs in VPS35-KO or VPS35-OE and parental MHCC-97H or Huh7 cells, respectively (Fig. 3B). Wnt/PCP signaling plays important roles in metastasis; therefore, we investigated if *VPS35* promoted migration, invasion, and EMT via the activation of Wnt/PCP pathway in HCC cells. Overexpression of *VPS35* in Huh7 cells reduced phosphorylation of RhoA at Ser188, Rac at Ser71 and p62 at Serine 403, while simultaneously increasing the expression of p62 and Rock1 and phosphorylation of JNK (Fig. 3C). Knockout of *VPS35* in MHCC-97H cells showed the opposite effect (Fig. 3C). Wound scratch assays (Fig. 3D) and transwell assays (Fig. 3E) confirmed that the ROCK inhibitor GSK269962A can suppress VPS35-induced HCC cell migration and invasion. These results indicate that VPS35 might induce cell migration, invasion, and EMT through activation of Wnt/PCP signaling pathway.

VPS35 activates Wnt/PCP signaling pathway by regulating the sorting and trafficking of FZD2 and ROR1 to the plasma membrane

VPS35 directly associates with sorting signal cargo proteins.[17] We next investigated the potential cytosolic retrieval

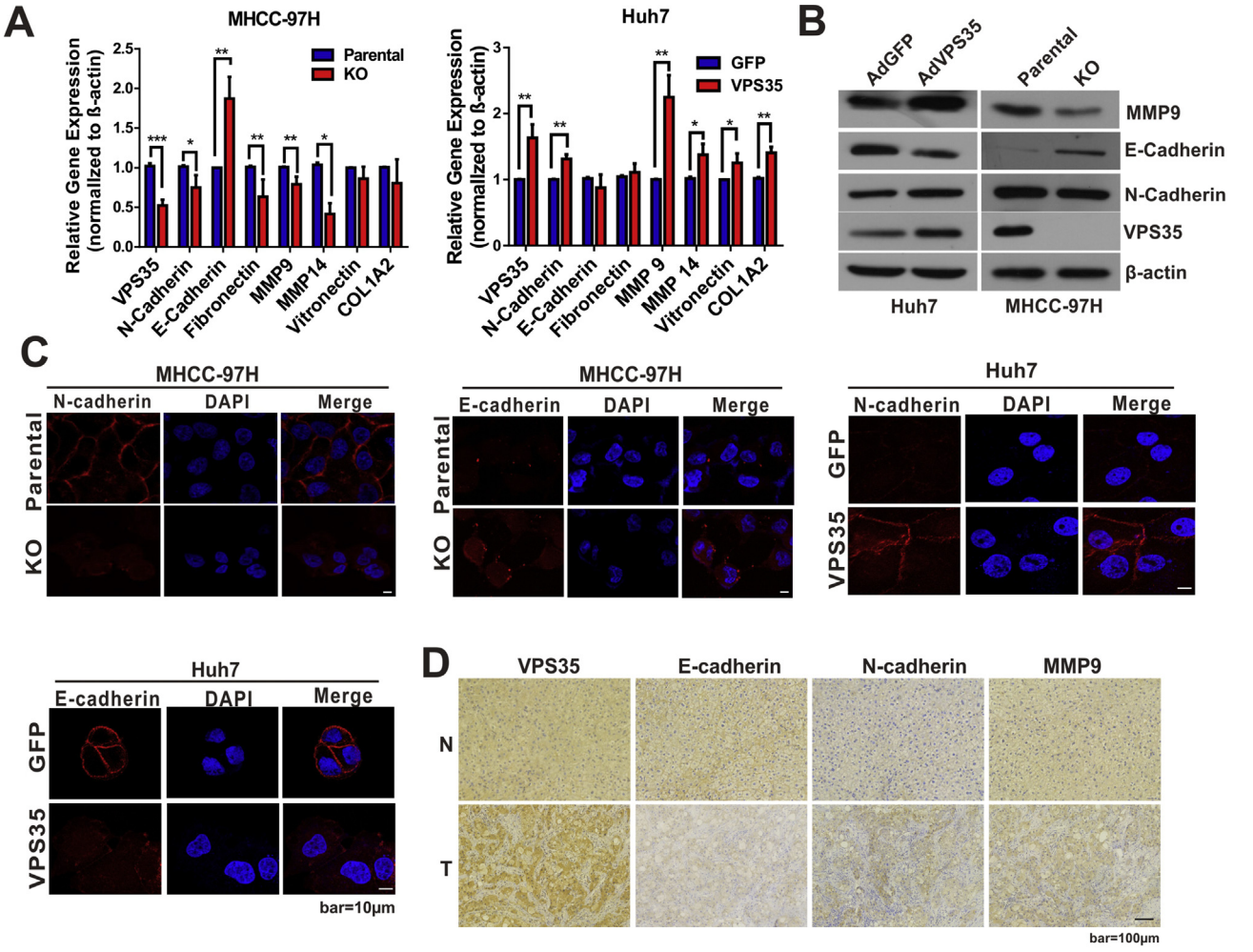

Figure 2 VPS35 knockout reduces the expression of EMT-related genes in hepatoma cells. (**A**) The mRNA expression levels of EMT-related genes in VPS35-OE and VPS35-KO cells were detected by quantitative real-time PCR. Data are means ± SD. ($n = 3$, performed in triplicate). $^{*}P < 0.05$, $^{**}P < 0.01$; $^{***}P < 0.001$. The protein expression of E-cadherin, N-cadherin, and MMP9 in hepatoma cells were examined by (**B**) western blotting and (**C**) immunofluorescence. Nuclei were counterstained with DAPI. (**D**) Immunohistochemical staining of normal (N) and tumor (T) tissues with anti-VPS35, anti-E-cadherin, anti-MMP9, and anti-N-cadherin antibodies.

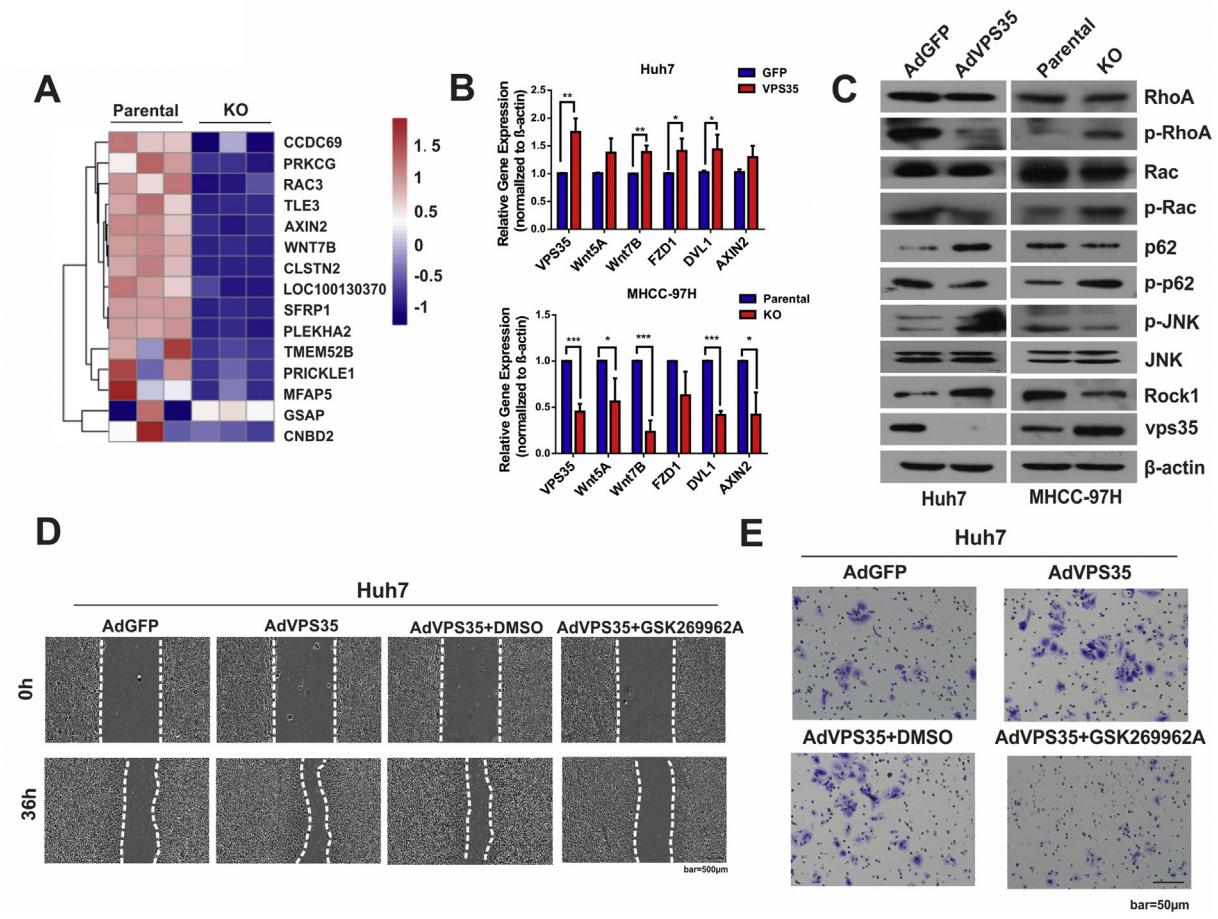

Figure 3 Overexpression of VPS35 activates Wnt/PCP signaling pathway in hepatoma cells. (**A**) Heatmap showing the differentially expressed genes of Wnt pathway in VPS35-deficient and parental SK-Hep1 cells. (**B**) The mRNA expression of Wnt-related genes in VPS35-KO or parental MHCC-97H and VPS35-OE or parental Huh7 cells were examined by quantitative real-time RT-PCR. β-actin was used as an internal control. All experiments were performed in triplicate. Data are means ± SD. $^{*}P < 0.05$, $^{**}P < 0.01$; $^{***}P < 0.001$. (**C**) The protein levels of Wnt/PCP signaling-related makers were examined by immunoblot. Wound scratch assays (**D**) and transwell assays (**E**) with *VPS35*-OE Huh7 cells treated with ROCK inhibitor GSK269962A (10 nM) for 36 h.

proteins related to VPS35. Through global proteomic analysis *in vitro* and in non-polarized cultured cells, FRIZZLED-2 (FZD2) and ROR1 were regulated by VPS35, respectively.[18] Therefore, we assumed that *VPS35* activated the Wnt/PCP signaling by regulating the intracellular localization of FZD2 and ROR1. Consistently, immunoblots revealed a marked decrease in cell-surface FZD2 and ROR1 in VPS35-KO MHCC-97H cells, whereas overexpression of *VPS35* increased the levels of cell-surface FZD2 and ROR1 (Fig. 4A). Immunofluorescence confirmed a substantial reduction in membrane localization of ROR1 in *VPS35*-KO cells, indicating a decreased recycling of ROR1. Conversely, *VPS35*-OE cells showed the opposite effect (Fig. 4B). Next, we analyzed *VPS35* expression in clinical HCC samples and explored the potential association between expression of *VPS35*, *FZD2*, and *ROR1* in HCC tissues. In an independent cohort of 371 HCC samples from the Cancer Genome Atlas (TCGA) database, *VPS35* expression was positively correlated with *ROR1* expression ($r = 0.4702$, $P < 0.0001$; Fig. 4C). To confirm these data, we analyzed the expression of these proteins in 16 HCC specimens and adjacent non-cancerous specimens. Immunoblot analysis showed that *VPS35* expression was dramatically upregulated in tumor samples (Fig. 4D). Notably, in most cases, a higher expression of *VPS35* was associated with higher expression of Wnt receptors FZD2 and ROR1, which indicated the potential important roles of *VPS35* played in HCC metastasis (Fig. 4D). Taken together, these results demonstrated that VPS35 activated the Wnt/PCP signaling through sorting and trafficking of FZD2 and ROR1 to the plasma membrane in hepatoma cells.

Discussion

In our previous study, we identified VPS35 as a novel potential oncogene in HCC. We showed that VPS35 is upregulated in HCC tissues and indicates a poor prognosis for patients with HCC. Furthermore, the overexpression of VPS35 promotes the proliferation of HCC cells by activating the PI3K/AKT signaling pathway.[15] However, its potential function in the metastasis of HCC was thus far poorly understood. In this study, we found that VPS35 overexpression promotes HCC cell migration and invasion *in vivo* and *in vitro* and accelerates EMT progression by activating the

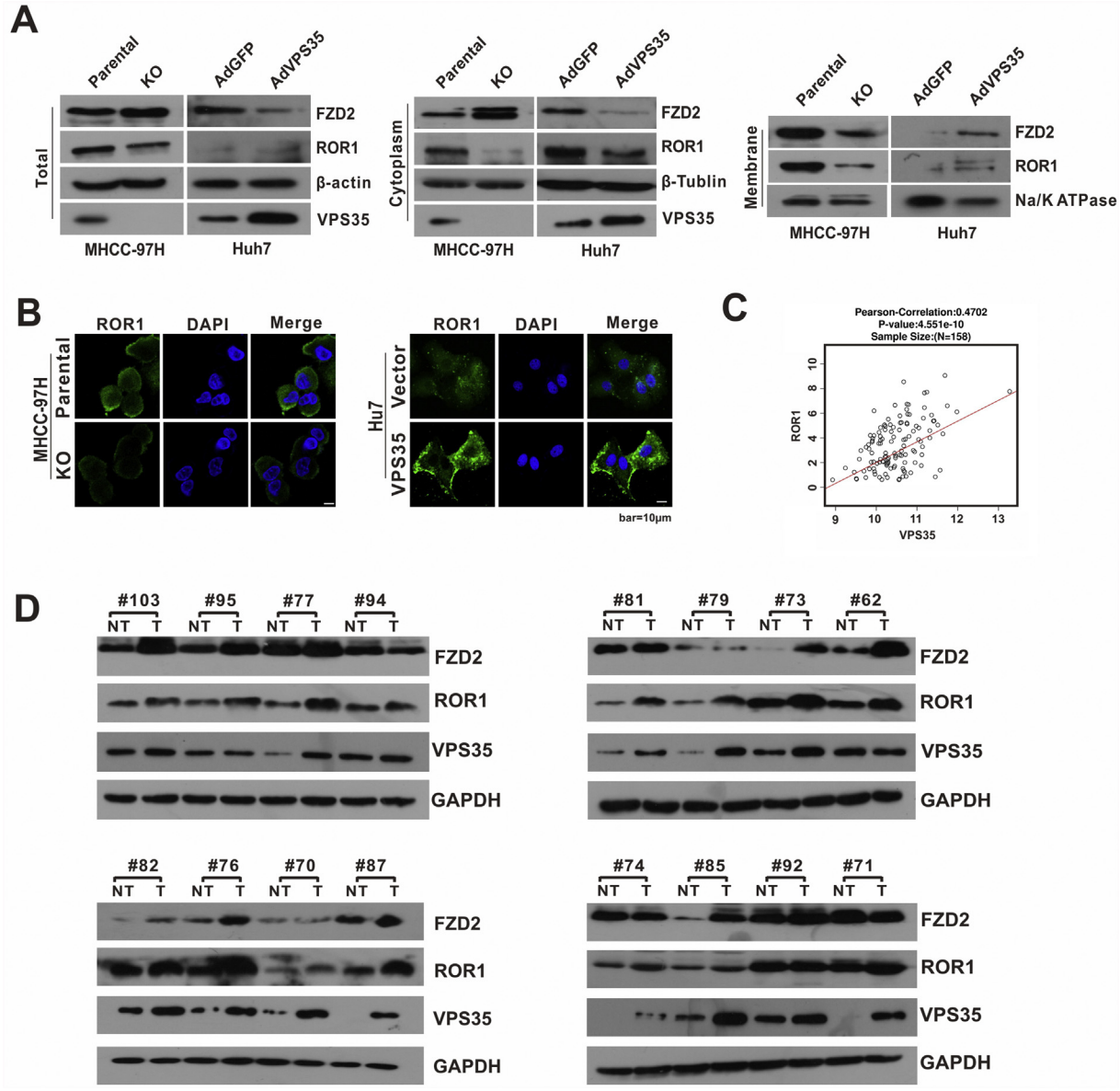

Figure 4 VPS35 activates Wnt/PCP signaling pathway via regulating the sorting and trafficking of FZD2 and ROR1 to the plasma membrane. (**A**) Western blot analysis of FZD2 and ROR1 expression in total cell lysates or cytoplasm and plasma membrane fractions in HCC cells. β-actin, β-Tubulin and Na/K ATPase served as quality control for total, cytoplasmic, and membrane protein extraction, respectively. (**B**) Immunofluorescent staining of ROR1 in VPS35-KO or parental MHCC-97H and VPS35-OE Huh7 cells. Nuclei were stained with DAPI. (**C**) Bioinformatic analysis of correlation between *ROR1* and *VPS35* expression. Correlation among *ROR1* and *VPS3*5 mRNA based on data from the TCGA LIHC database. Statistical analysis was performed using Pearson's correlation coefficient ($P < 0.0001$). (**D**) The protein expression levels of VPS35, ROR1, and FZD2 in 16 paired HCC (T) and non-tumor (NT) liver tissues.

Wnt/PCP signaling pathway. Mechanistically, VPS35 activates the Wnt/PCP pathway by regulating the sorting and trafficking of FZD2 and ROR1.

The EMT of neoplastic hepatocytes is a key event in metastasis.[19] Several studies have reported the role of the retromer complex in regulation of membrane proteins involved in EMT. VPS35 is the central cargo-binding subunit of the retromer complex.[20] Similar to the classical retromer cargoes, membrane proteins are also regulated by the retromer complex. Crumbs (Crb), a key polarity protein in EMT, is a retromer cargo that interacts with VPS35.[21] Moreover, several members of the SNX family in the retromer pathway can regulate intracellular trafficking of E-cadherin[22] Here, we found that VPS35 upregulated MMP9 and N-cadherin, but downregulated E-cadherin. Conversely, VPS35 depletion upregulated E-cadherin, but downregulated MMP9 and N-cadherin. Therefore, we proposed that VPS35 promotes HCC cell migration and invasion by inducing EMT. However, the detailed transport mechanism of the three key EMT markers mediated by VPS35 needs to be further studied.

Our transcriptomic studies indicate that VPS35 deficiency inhibits Wnt/PCP signaling pathway in HCC cells. The

Wnt/PCP pathway regulates actin cytoskeleton remodeling, cellular invasion, and migration through small GTPases of the Rho family (Rac1, RhoA, Cdc42) and the JNK pathway.[23] Previous studies showed that Vps35 regulates either the activity or the expression of Rac1 in *Drosophila*.[24] In this study, we demonstrated that VPS35 reduces phosphorylation of Rac at Ser 71, thereby regulating its activity. VPS35 also upregulated the activity of RhoA and the expression of its downstream effector Rock1. Moreover, SQSTM1/p62 protein was reported as a novel VANGL2-binding partner in Wnt/PCP signaling.[25] Our study suggested that VPS35 upregulates p62 and p-JNK. Importantly, VPS35-promoted HCC invasion and migration were partially suppressed by the ROCK inhibitor GSK269962A, indicating that VPS35 exerts its oncogenic role via activation of Wnt/PCP pathway.

Recognition and selection of signaling receptors (e.g., *IFNAR2* and *TβRII*) by VPS35 has been widely studied.[26,27] Previous studies suggested that the retromer complex is involved in Wnt signaling pathway.[28] Vps35 loss significantly reduces Wnt secretion in *Caenorhabditis elegans*, *Drosophila*, and mammalian cultured cells. Since VPS35 interacts directly with the conserved transmembrane protein MIG-14/Wls, it retrieves endocytosed Wls from the endosome to the TGN, after which Wls is reused for further Wnt secretion.[29] In this study, we demonstrated that VPS35 participates in non-canonical Wnt signaling. The membrane distribution of FZD2 and ROR1 was increased in VPS35-OE Huh7 cells, while it was markedly reduced VPS35-KO MHCC-97H cells. These findings indicate that VPS35 might facilitate the recycling of membrane-localized FZD2 and ROR1, thus promoting the activation of downstream Wnt/PCP signaling. We assumed that the increased membrane recycling and/or decreased lysosomal degradation of FZD2 and ROR1 could contribute to the increased levels of these proteins in VPS35-OE cells, which in turn might boost the activation of the Wnt/PCP signaling. However, the detailed molecular mechanism by which VPS35 mediates FZD2 and ROR1 recycling remains to be further investigated.

In summary, the present work is the first to reveal that VPS35 promotes HCC cell metastasis and mediates EMT by activating the Wnt/PCP signaling pathway. These results further broaden our understanding of the role of VPS35 in EMT process and HCC metastasis. Our study may facilitate the evaluation of VPS35 as a potential prognostic biomarker of HCC, as well as offer a new therapeutic target in HCC metastasis therapy.

Conflict of Interests

The authors have no financial conflict of interest.

Acknowledgements

We would like to thank Dr. Tong-Chuan He (University of Chicago, USA) for providing the pAdEasy plasmid system. This work was supported by National Natural Science Foundation of China (grant numbers 81872270 and 81572683 to NT), the Natural Science Foundation Project of Chongqing (cstc2019jcyj-msxmX0587 to KW), the Science and Technology Research Program of Chongqing Municipal Education Commission (Grant number KJQN201900429 to KW), the Major National S&T program (2017ZX10202203-004 to NT), Natural Science Foundation Project of CQ CSTC (cstc2018jcyjAX0254 to NT), and the Leading Talent Program of CQ CSTC (CSTCCXLJRC201719 to NT).

Appendix A. Supplementary data

Supplementary data to this article can be found online at https://doi.org/10.1016/j.gendis.2020.07.009.

References

1. Forner A, Reig M, Bruix J. Hepatocellular carcinoma. *Lancet*. 2018;391(10127):1301—1314.
2. Bray F, Ferlay J, Soerjomataram I, Siegel RL, Torre LA, Jemal A. Global cancer statistics 2018: GLOBOCAN estimates of incidence and mortality worldwide for 36 cancers in 185 countries. *CA Cancer J Clin*. 2018;68(6):394—424.
3. Llovet JM, Zucman-Rossi J, Pikarsky E, et al. Hepatocellular carcinoma. *Nat Rev Dis Prim*. 2016;2(1),e16018.
4. Mazzoccoli G, Tarquini R, Valoriani A, Oben J, Vinciguerra M, Marra F. Management strategies for hepatocellular carcinoma: old certainties and new realities. *Clin Exp Med*. 2016;16(3):243—256.
5. Niehrs C. The complex world of WNT receptor signalling. *Nat Rev Mol Cell Biol*. 2012;13(12):767—779.
6. Milgrom-Hoffman M, Humbert PO. Regulation of cellular and PCP signalling by the scribble polarity module. *Semin Cell Dev Biol*. 2018;81:33—45.
7. VanderVorst K, Hatakeyama J, Berg A, Lee H, Carraway KL. Cellular and molecular mechanisms underlying planar cell polarity pathway contributions to cancer malignancy. *Semin Cell Dev Biol*. 2018;81:78—87.
8. VanderVorst K, Dreyer CA, Konopelski SE, Lee H, Ho H-YH, Carraway KL. Wnt/PCP signaling contribution to carcinoma collective cell migration and metastasis. *Cancer Res*. 2019;79(8):1719—1729.
9. O'Connell MP, Fiori JL, Xu M, et al. The orphan tyrosine kinase receptor, ROR2, mediates Wnt5A signaling in metastatic melanoma. *Oncogene*. 2010;29(1):34—44.
10. Gujral TS, Chan M, Peshkin L, Sorger PK, Kirschner MW, MacBeath G. A noncanonical Frizzled2 pathway regulates epithelial-mesenchymal transition and metastasis. *Cell*. 2014;159(4):844—856.
11. Asad M, Wong M, Tan T, et a l. FZD7 drives in vitro aggressiveness in stem-A subtype of ovarian cancer via regulation of non-canonical Wnt/PCP pathway. *Cell Death Dis*. 2014;5(7),e1346.
12. Williams ET, Chen X, Moore DJ. VPS35, the retromer complex and Parkinson's disease. *JPD*. 2017;7(2):219—233.
13. Wang S, Bellen HJ. The retromer complex in development and disease. *Development*. 2015;142(14):2392—2396.
14. Zhou M, Wiener H, Su W, et al. VPS35 binds farnesylated N-Ras in the cytosol to regulate N-Ras trafficking. *J Cell Biol*. 2016;214(4):445—458.
15. Zhang Guiji, Tang Xia, Liang Li, et al. DNA and RNA sequencing identified a novel oncogene VPS35 in liver hepatocellular carcinoma. *Oncogene*. 2020;39(16):3229—3244.
16. Hugo H, Ackland ML, Blick T, et al. Epithelial—mesenchymal and mesenchymal—epithelial transitions in carcinoma progression. *J Cell Physiol*. 2007;213(2):374—383.
17. Vergés M. Retromer in polarized protein transport. *Int Rev of Cell Mol Bio*. 2016;323:129—179.

18. Steinberg F, Gallon M, Winfield M, et al. A global analysis of SNX27—retromer assembly and cargo specificity reveals a function in glucose and metal ion transport. *Nat Cell Biol*. 2013;15(5):461—471.
19. Lamouille S, Xu J, Derynck R. Molecular mechanisms of epithelial—mesenchymal transition. *Nat Rev Mol Cell Biol*. 2014;15(3):178—196.
20. Williams ET, Chen X, Moore DJ. VPS35, the retromer complex and Parkinson's disease. *J Parkinsons Dis*. 2017;7(2): 219—233.
21. Pocha SM, Wassmer T, Niehage C, Hoflack B, Knust E. Retromer controls epithelial cell polarity by trafficking the apical determinant crumbs. *Curr Biol*. 2011;21(13):1111—1117.
22. Xu J, Zhang L, Ye Y, et al. SNX16 regulates the recycling of E-cadherin through a unique mechanism of coordinated membrane and cargo binding. *Structure*. 2017;25(8):1251—1263.
23. Katoh M. WNT/PCP signaling pathway and human cancer (review). *Oncol Rep*. 2005;14(6):1583—1588.
24. Korolchuk VI, Schutz MM, Gomez-Llorente C, et al. Drosophila Vps35 function is necessary for normal endocytic trafficking and actin cytoskeleton organisation. *J Cell Sci*. 2007;120(24): 4367—4376.
25. Puvirajesinghe TM, Bertucci F, Jain A, et al. Identification of p62/SQSTM1 as a component of non-canonical Wnt VANGL2—JNK signalling in breast cancer. *Nat Commun*. 2016; 7(1),e10318.
26. Yin X, Murphy SJ, Wilkes MC, Ji Y, Leof EB. In: Heldin C-H, ed. *Retromer Maintains Basolateral Distribution of the Type II TGF-b Receptor via the Recycling Endosome*. *Mol Biol Cell*. 2013;24(14):2285—2298.
27. Cui Y, Carosi JM, Yang Z, et al. Retromer has a selective function in cargo sorting via endosome transport carriers. *J Cell Biol*. 2019;218(2):615—631.
28. Prasad BC. Wnt signaling establishes anteroposterior neuronal polarity and requires retromer in *C. elegans*. *Development*. 2006;133(9):1757—1766.
29. Yang P-T, Lorenowicz MJ, Silhankova M, Coudreuse DYM, Betist MC, Korswagen HC. Wnt signaling requires retromer-dependent recycling of MIG-14/Wntless in Wnt-producing cells. *Dev Cell*. 2008;14(1):140—147.